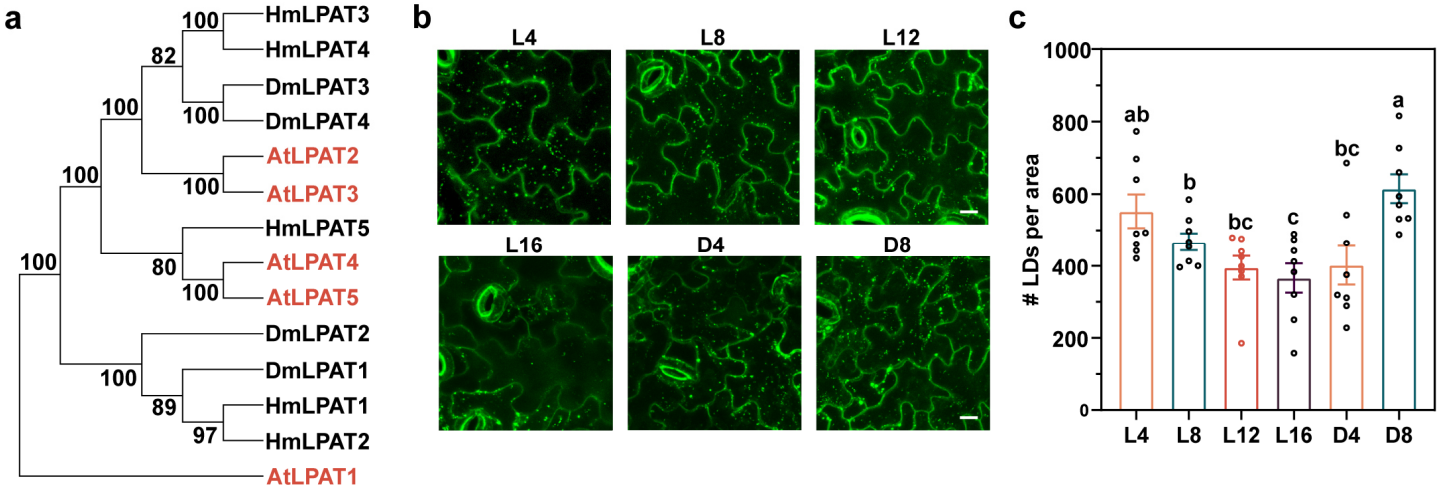

Extended Data Fig. 1. Photoperiod regulates the LD profile.

a, Clustering neighbor-joining tree showing the relatedness of LPATs from *Arabidopsis* (At) to *Drosophila* (Dm) and *Homo sapiens* (Hm) based on amino-acid sequence analysis. **b,** Confocal micrographs of LDs in WT leaves after light and dark treatments. *Arabidopsis* plants were cultured over a typical day/night growth cycle (16 h light/8 h dark), and LDs were observed (L, light; D, dark). Bars, 10 μm. **c,** LD number in leaves treated as in (b). Data are means ± SEM of two micrographs of two leaf samples from four individual plants. Different letters indicate significant differences as determined by two-sided Student's *t*-test ($P < 0.05$).

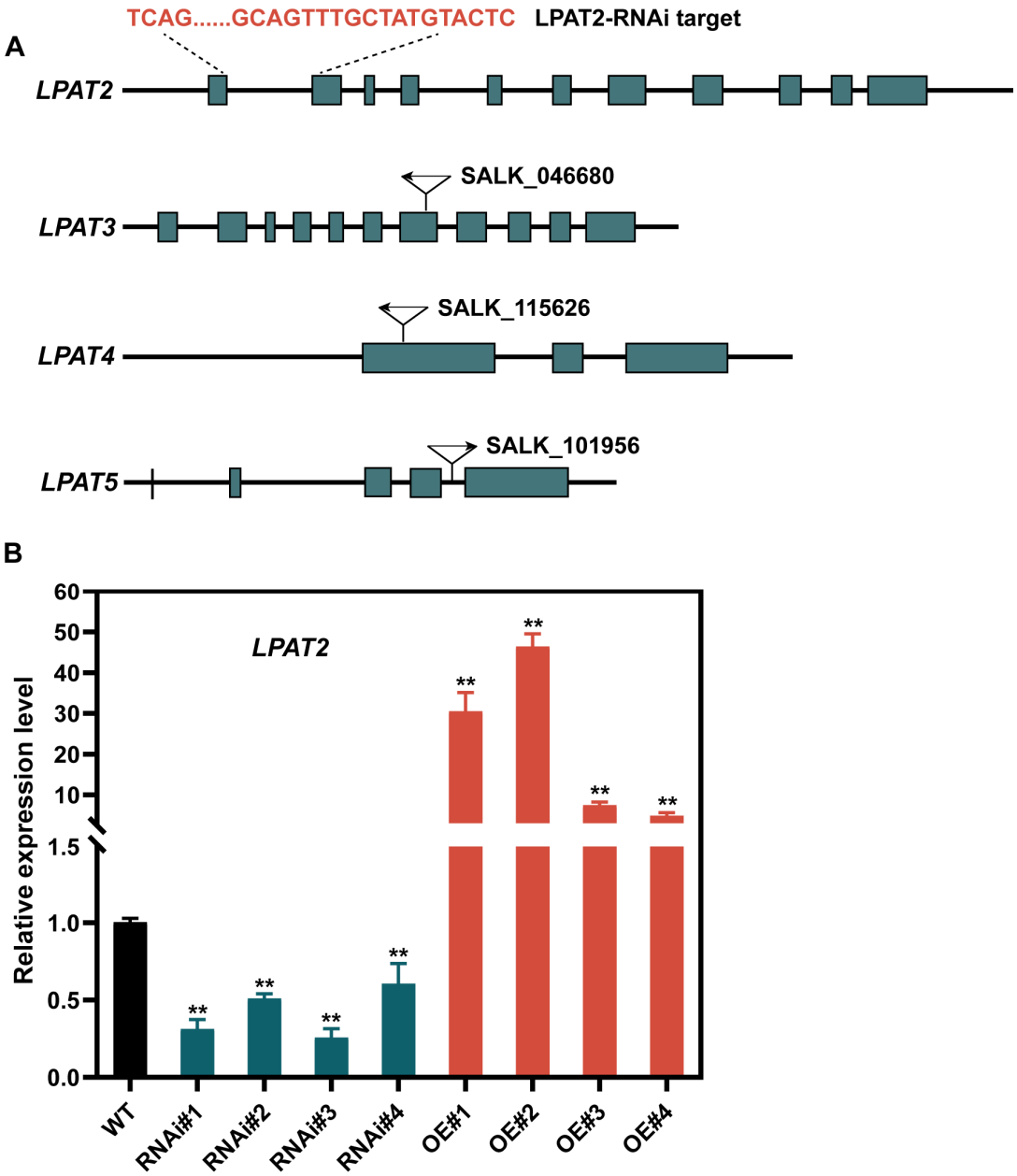

Extended Data Fig. 2. Identification of *lpat* mutants and LPAT2-OE transgenic lines.

a, Schematic of the target sequence for the LPAT2-RNAi knockdown line and the sites of T-DNA insertion in *LPAT3/4/5*. **b,** RT-qPCR analysis of *LPAT2* expression in rosette leaves of the WT, LPAT2-RNAi, and OE lines. Data are means ± SEM from at least four individual plants per line (n = 8). RNAi#1 and OE#1 were used for further analysis. Statistical significance between the WT and each transgenic line was analyzed by Student's *t*-test (*P < 0.05, **P < 0.01).

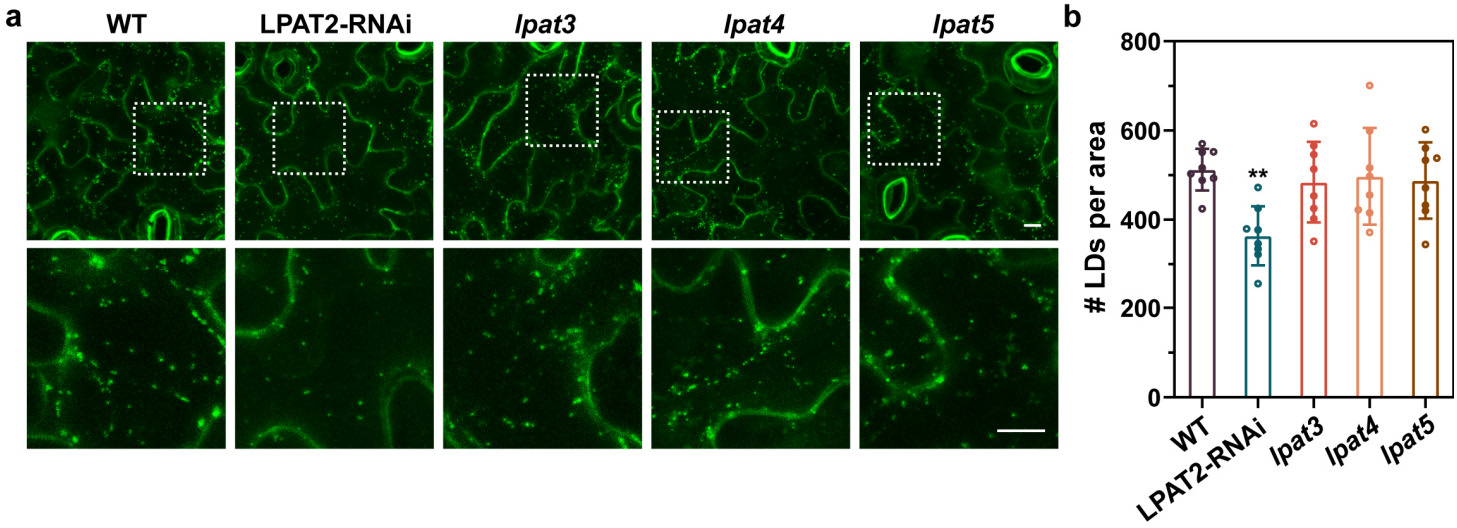

Extended Data Fig. 3. Dark-induced LD abundance in the *lpat* mutants.

a, Confocal micrographs of dark (8 h)-induced LDs in the leaves of WT, LPAT2-RNAi, *lpat3*, *lpat4*, and *lpat5*. Bars, 10 μm. **b,** LD number according to the treatments in (a). Data are means ± SEM from at least four individual plants per line (n = 8). Statistical analysis was performed by two-sided Student's *t*-test (*P < 0.05, **P < 0.01).

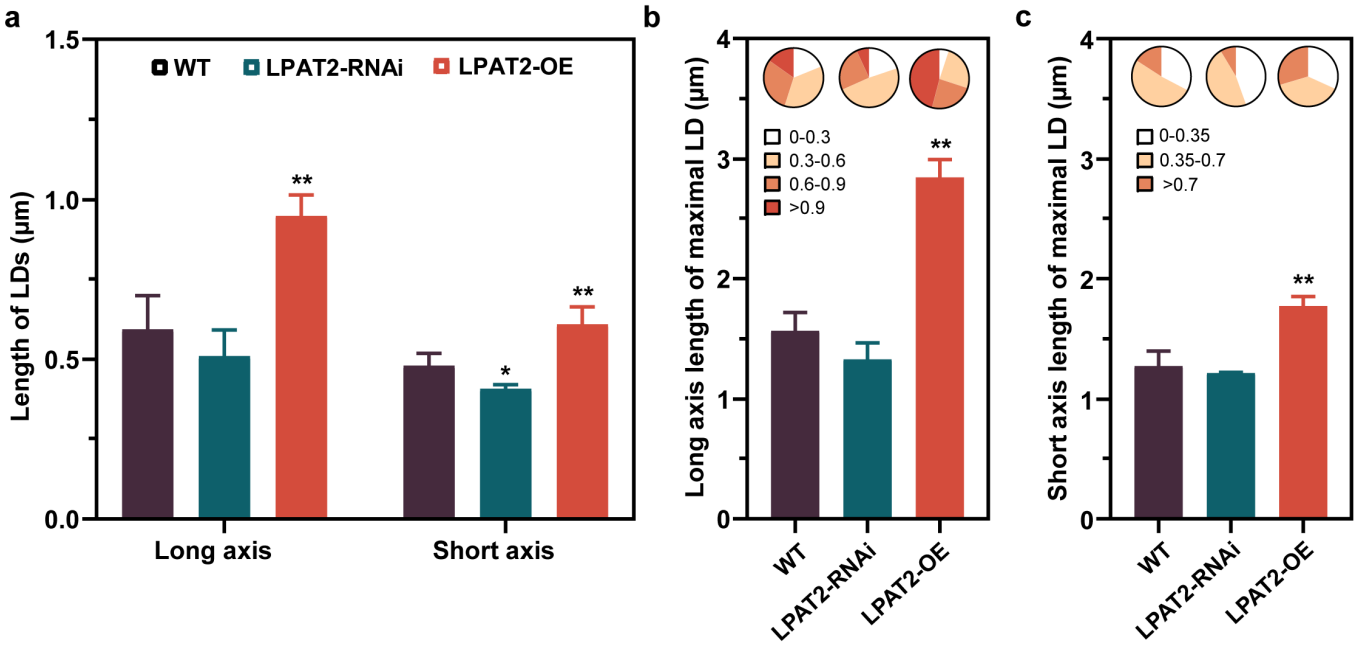

Extended Data Fig. 4. LPAT2 regulates the morphology and size of seed LDs.

LD sizes in seeds of the WT, LPAT2-RNAi, and OE lines, in terms of length (a), long axis length (b), and short axis length of the maximal LD (c). LDs were counted in three individual cells of WT (n = 504 LDs), LPAT2-RNAi (n = 732 LDs) and LPAT2-OE (n = 523 LDs). Data are means ± SEM. Statistical analysis was performed by two-sided Student's *t*-test (*P < 0.05, **P < 0.01).

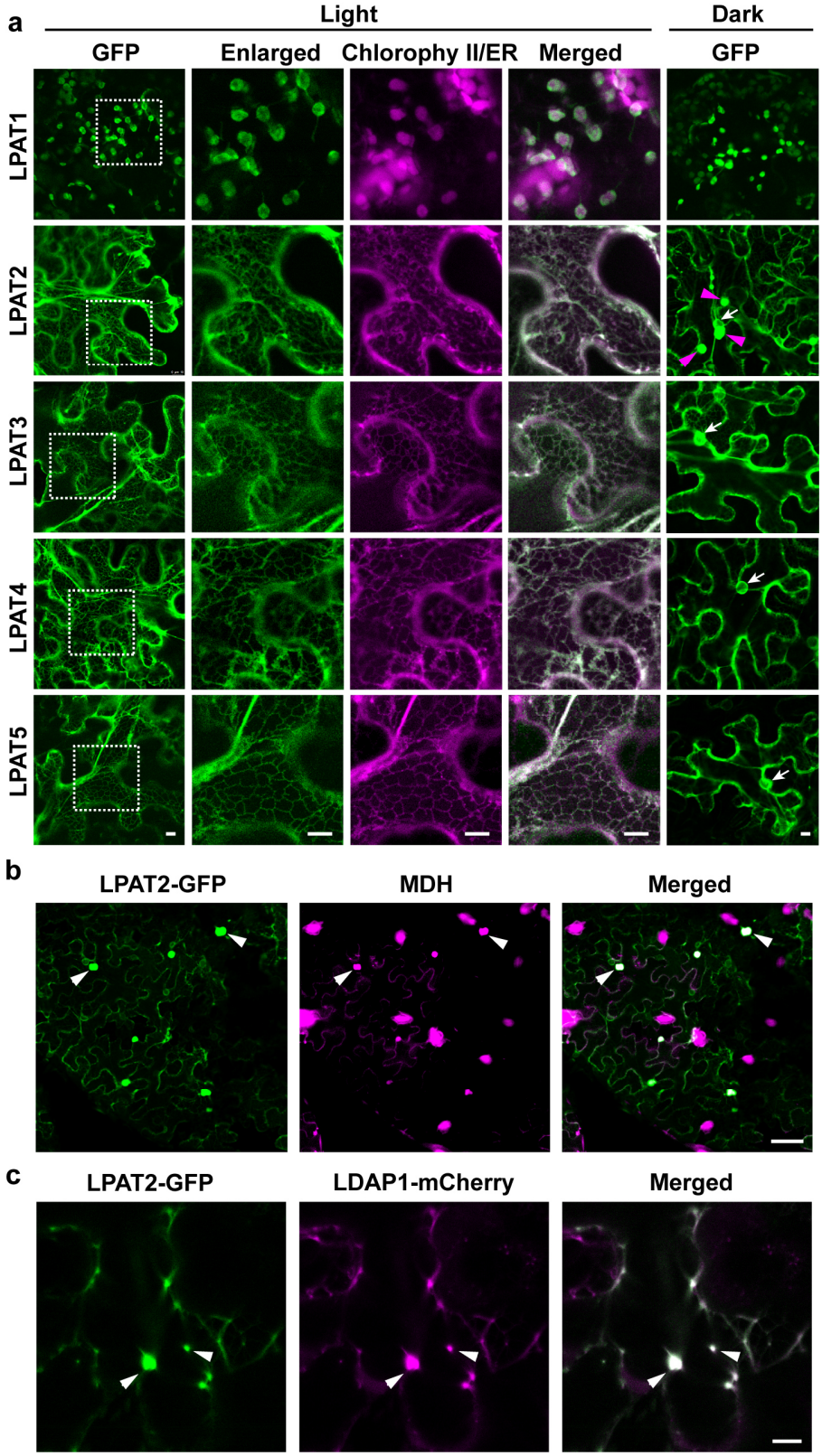

Extended Data Fig. 5. Subcellular localization of LPATs in *N. benthamiana* leaves.

a, Subcellular targeting of *Arabidopsis* LPATs in *N. benthamiana*. LPATs tagged with GFP at the C-terminus were transiently expressed in *N. benthamiana* leaves with or without the ER maker mCherry-HDEL for 3 d before confocal observation. *N. benthamiana* leaves expressing LPAT-GFP were incubated under dark conditions for 3 d. Bars = 10 μm. **b,** LPAT2-GFP colocalizes with monodansylpentane (MDH)-stained LDs in *N. benthamiana* leaves. Bar, 50 μm. **c,** LPAT2-GFP colocalizes with LDAP1-mCherry in *N. benthamiana* leaves. Bar, 5 μm.

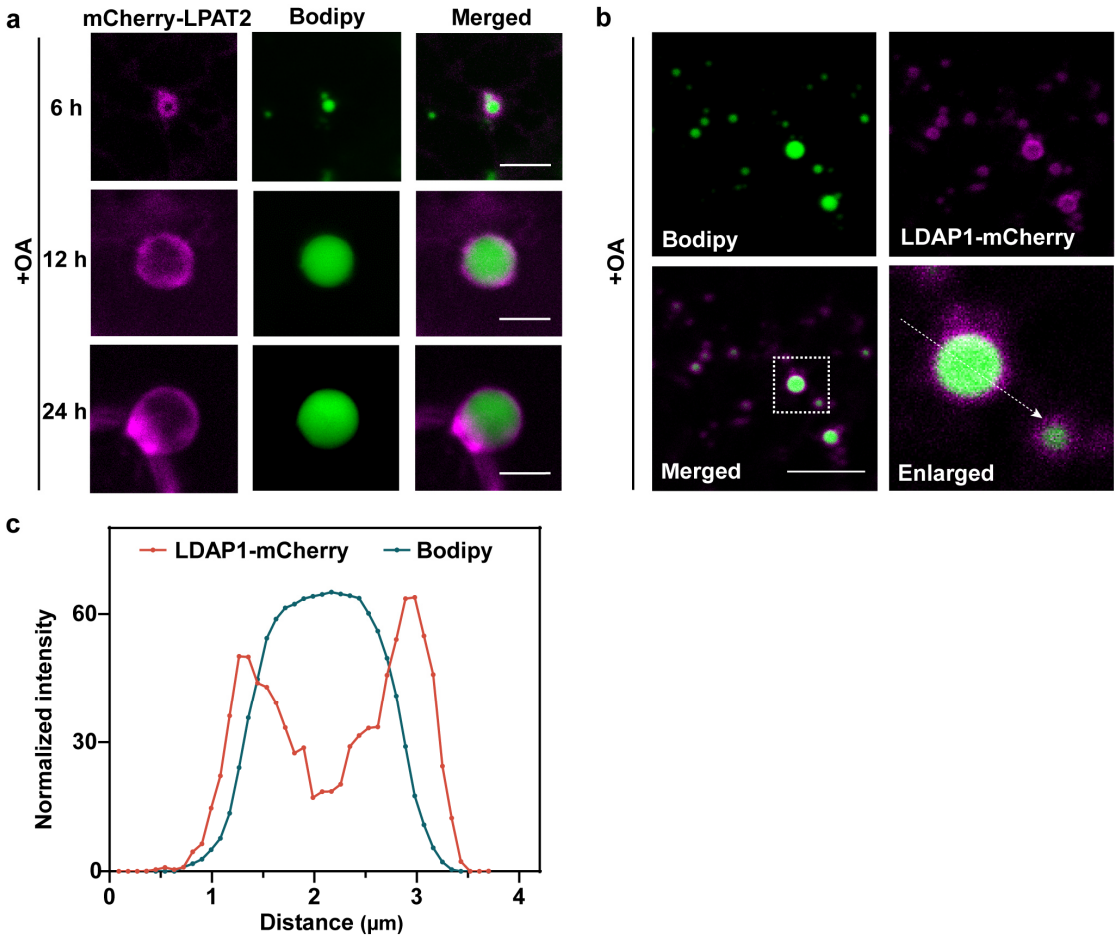

Extended Data Fig. 6. LPAT2 and LDAP1 localized to the surface of LDs.

a, mCherry-LPAT2-expressing *Arabidopsis* leaves were treated with 200 μM OA for 6, 12, and 24 h to induce LD formation. LDs were stained with Bodipy. Bar, 5 μm. **b,** LDAP1-mCherry localized to the LD surface upon OA treatment. LDAP1-mCherry-expressing *Arabidopsis* leaves were treated with 200 μM OA for 8 h to induce LD formation before Bodipy staining. Bar, 5 μm.

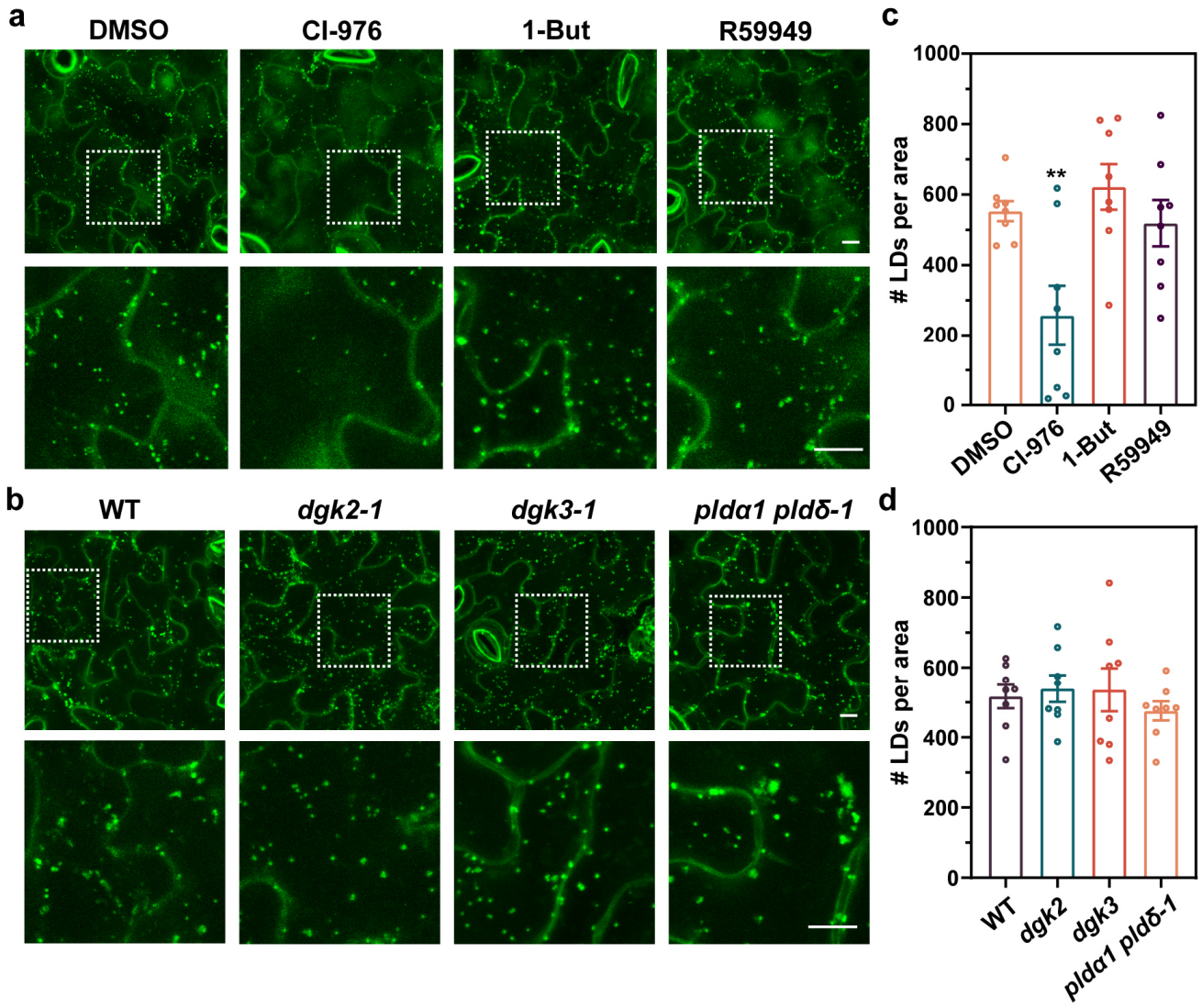

Extended Data Fig. 7. LPAT2-derived PA is involved in the regulation of LD formation.

a, Confocal micrographs of dark-induced LDs in WT leaves exposed to dark with or without an inhibitor treatment. *Arabidopsis* plants were transferred to half-strength MS medium with CI-976 (50 μM), 0.1% (v/v) 1-But, and R59949 (12.5 μM) before exposure to darkness for 8 h. Bars, 10 μm. **b,** Confocal micrographs of dark-induced LDs in WT, *pldα1 pldδ-1*, *dgk2-1*, and *dgk3-1*. Bars, 10 μm. **c,** LD numbers in WT leaves treated as in (a) (n = 8 from 4–5 leaves). Data are means ± SEM. Statistical significance was analyzed by Student's *t*-test (*P < 0.05, **P < 0.01). **d,** LD numbers in the leaves of WT, *dgk2-1*, *dgk3-1*, and *pldα1 pldδ-1* (n = 8 from 4–5 leaves). Data are means ± SEM. Statistical significance between WT and each mutant line was analyzed by Student's *t*-test (*P < 0.05, **P < 0.01).

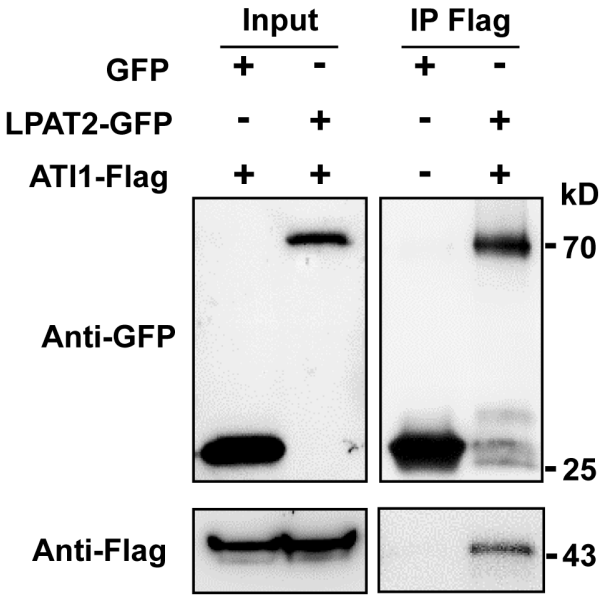

Extended Data Fig. 8. ATI1 coimmunoprecipitated with LPAT2 in *N. benthamiana* leaves.

LPAT2-GFP or GFP was coexpressed with ATI1-Flag in *N. benthamiana* and subjected to anti-Flag IP. Proteins were subjected to immunoblotting using anti-Flag and anti-GFP antibodies.

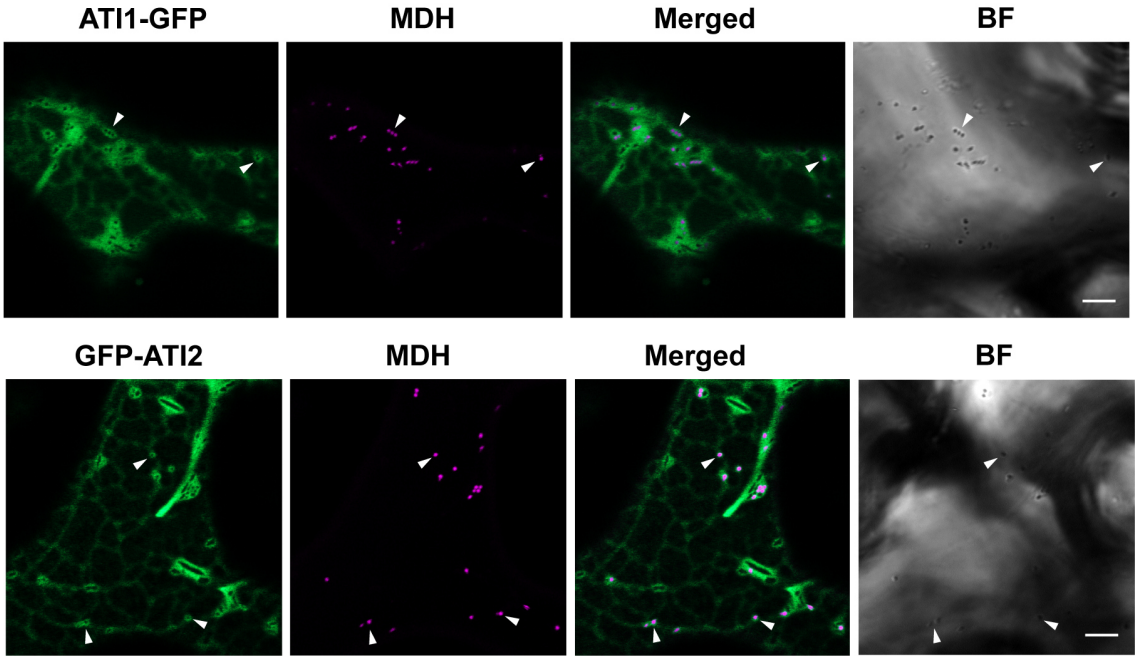

Extended Data Fig. 9. ATI1/2 localized to the surface of dark-induced LDs.

ATI1-GFP-expressing and GFP-ATI2-expressing *Arabidopsis* leaves were incubated under dark conditions for 8 h to induce LD formation and stained with MDH. Bars, 5 μm.